Organic field-effect transistors of poly(2,5-bis(3-dodecylthiophen-2-yl)-thieno[2,3-*b*]thiophene) deposited on five different silane self-assembled monolayers†

Ruth Rawcliffe,[a] Maxim Shkunov,[bc] Martin Heeney,[d] Steven Tierney,[b] Iain McCulloch[e] and Alasdair Campbell*[a]

Received (in Cambridge, UK) 9th October 2007, Accepted 6th December 2007
First published as an Advance Article on the web 21st December 2007
DOI: 10.1039/b715536k

Depositing a fused-ring thieno-thiophene polymer on different self-assembled monolayers indicates that varying the SAM surface energy changes the FET mobility and turn-on voltage by varying polymer crystallinity at the buried interface.

Polymer field-effect transistors (FETs) are one of the most exciting developing technologies, allowing the fabrication by printing techniques of lightweight, flexible displays and many other devices.[1–4] Using silane self-assembled monolayers (SAMs) in the channel, such as octadecyltrichlorosilane and hexamethyldisilazene, has been shown to improve the performance of bottom-gate polymer FETs.[5–10] In poly(3-hexylthiophene) (P3HT) improvements in mobility can be directly linked to the chain packing and orientation and the crystallinity at the semiconductor–insulator interface.[6–8] This may be due to both an improvement in substrate planarity and P3HT formulation wettability.[5,7] Thermally evaporated pentacene FETs have also been shown to have increased crystal grain size and better molecular orientation when deposited on silane SAMs, with a resultant improvement in mobility and turn-on voltage.[5,11–13]

Here we investigate the effect of five different silane SAMs on bottom-gate FETs of poly(2,5-bis(3-dodecylthiophen-2-yl)-thieno[2,3-*b*]thiophene) (pBTCT) (Fig. 1).[14] This is a fused ring thieno-thiophene polymer with a maximum reported mobility of 0.15 $cm^2\ V^{-1}\ s^{-1}$ which is stable in ambient atmosphere and light. The *ant* variant has been shown to have an even higher maximum value of 0.6 $cm^2\ V^{-1}\ s^{-1}$.[15] The SAMs investigated were octadecyltrichlorosilane (ODTS), octyltrichlorosilane (OTS), 1,1,1,3,3,3-hexamethyldisilazene (HMDS), phenyltrichlorosilane (PETS) and (3-aminopropyl)-triethoxysilane (APTS) (Fig. 2).

The saturation regime transfer characteristics of pBTCT FETs with the five silane SAMs are shown in Fig. 3. The performance parameters for these devices are listed in Table 1, along with values for a reference device containing no SAM where the polymer solution was deposited on the bare SiO_2 insulator surface. For the SAM devices, the maximum current follows $I_{ODTS} > I_{OTS} > I_{HMDS} > I_{PETS} > I_{APTS}$. The saturation mobility follows the same relationship, increasing by a factor of $\times 420$ from APTS to ODTS. All except APTS give an improved mobility over the reference device. Therefore, the choice of SAM can have a dramatic effect on the mobility, which also results in a higher ON current and ON/OFF ratio.

It has been reported that APTS produces better transport in P3HT devices than HMDS.[8] This is believed to be due to the amino end groups, which interact with the P3HT backbone and allow the sidechains to penetrate the SAM layer and interdigitate with the spacer groups, resulting in much better crystal orientation at the interface. Surprisingly, given the similarities in structure between P3HT and pBTCT, we do not see such an improvement in the present study, the amino SAM giving the worst performance. To investigate this further we tried to replicate the literature findings, but found P3HT FETs with APTS gave very poor performance. Given the extreme care taken in the current study to ensure good SAM coverage, we conclude that if any interdigitation effects do occur it is more to do with holes in the SAM layer than the chemical nature of the end groups.

The contact resistance R_C (TLM) is about the same for ODTS, OTS and HMDS, but is much larger for PETS. For APTS it is too large to be measured. Therefore, for large changes in mobility, R_C seems to increase with decreasing μ_{SAT}. Given that the same polymer and contacts are used, this suggests that there may be some carrier backflow mobility-limited injection in these devices as observed in organic light emitting diodes.[16] This is surprising as the crystallinity and

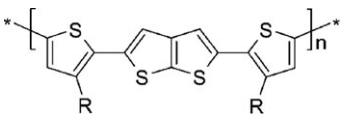

Fig. 1 Chemical structure of pBTCT (R = $-C_{12}H_{25}$).

[a] *Department of Physics, The Blackett Laboratory, Imperial College London, South Kensington Campus, London, UK SW7 2AZ. E-mail: alasdair.campbell@imperial.ac.uk*
[b] *Merck Chemicals, Chilworth Technical Centre, Southampton, UK*
[c] *Advanced Technology Institute, University of Surrey, Guildford, Surrey, UK GU2 7XH*
[d] *Department of Materials, Queen Mary, University of London, Mile End Road, London, UK E1 4NS*
[e] *Department of Chemistry, Imperial College London, South Kensington Campus, London, UK SW7 2AZ*

† Electronic supplementary information (ESI) available: Details of FET structure, substrate cleaning and preparation, SAM deposition, contact angle measurement, polymer molecular weight, polymer deposition, contact resistance and saturation mobility measurement and analysis. See DOI: 10.1039/b715536k

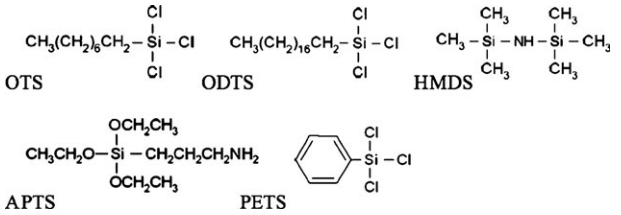

Fig. 2 Chemical structures of the silane SAMs used in this work.

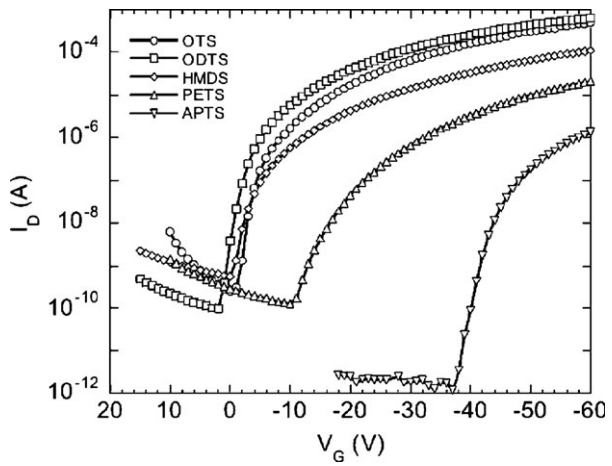

Fig. 3 Typical saturated regime transfer characteristics (at V_D = −60 V) for the polymer FETs (L = 20 μm) with different silane channel SAMs.

chain conformation and packing of pBTCT on the Au contacts should be identical. However, in this coplanar FET geometry charge injection into the polymer primarily occurs from the part of the source at the edge of the channel. It may be this which results in low values of the channel mobility affecting the contact resistance.

The contact angle of water on the surface of the different SAMs is listed in Table 1. This varies from 86° to 106°. The larger the contact angle, the more hydrophobic the SAM surface. Fig. 4 shows the variation of the saturation mobility of the SAM devices with contact angle. The mobility increases with increasing contact angle. This implies that the variations in mobility between the different SAMs are due to variations in the polymer physical structure created during deposition. The variations in SAM surface energy must result in changes in the orientation, conformation and packing of the polymer chains at the interface as they are deposited from dichlorobenzene and/or undergo the subsequent annealing step.

Similar measurements for P3HT support this relationship between SAM surface energy and morphology, but other results for poly(3,3‴-didodecylquaterthiophene) indicate that other factors can dominate in some solution processed polymers.[5,7,10]

To investigate the morphology at the buried interface, the variation of μ_{SAT} with temperature was measured from 294 to 354 K in 10 K steps for ODTS, OTS, HMDS and the reference device. Typical results are shown in Fig. 5 for an OTS device. The results were analyzed within the Gaussian disorder model (GDM) framework to obtain the energetic disorder parameter σ given by $\mu_{SAT} = \mu_0 \exp(-(2\sigma/3k_BT)^2)$.[17] This simple GDM

Table 1 pBTCT FET device parameters

SAM	Ref.	ODTS	OTS	HMDS	PETS	APTS
μ_{SAT}/cm^2 V^{-1} s^{-1}	0.0011	0.0210	0.0180	0.0050	0.0016	0.00005
R_C/MΩ cm[a]	—	0.51	0.48	0.49	2.1	$\ll 2$[b]
V_0/V	+1	+1	−1	0	−11	−38
Contact angle/°	—	106 ± 1	105 ± 1	94 ± 3	90 ± 3	86 ± 2
ON/OFF ratio	10^4	10^7	10^6	10^5	10^5	10^6
σ_{calc}/eV	0.057	0.052	0.053	0.058	—	—

[a] V_G = −40 V. [b] Can't measure—too large.

analysis assumes the zero-field approximation (usually valid for FETs as the source-drain field is typically much smaller than that found in diode structures) and that the temperature dependency of the mobility dominates over that of injection. The calculated values, σ_{calc}, must however be taken as an upper limit of the true value of σ. The results are listed in Table 1. For ODTS, OTS, HMDS and the reference device, the values of σ_{calc} are typical of a polycrystalline polymer.[18,19] They are also similar to the value of 0.54 eV reported for P3HT OTS FETs.[9] This indicates that transport in pBTCT is between ordered, polycrystalline grains. For ODTS, OTS and HMDS the mobility decreases with increasing energetic disorder. In the GDM this is associated with an increase in the width of the density of states (DOS) distribution which controls transport. For a polycrystalline material this can be associated with an increase in the depth of the typically exponential distribution of localized states which lie in the energy gap beneath the relatively iso-electronic crystal transport states. Such localized states physically occur at the grain boundaries, and for a polymer can be associated with isolated and relatively twisted and distorted chain segments between the ordered crystallites.

Insight into the effect of PETS and APTS on morphology can be gained from examining the FET turn-on voltage V_0. For the OTS, ODTS and HMDS devices V_0 is very low and close to zero volts. This suggests that these SAMs produce a very clean interface with little or no hole-trapping states. These FETs can be driven into hole accumulation mode at very small negative gate bias. This is not the case for PETS and APTS, which have very large and negative values of V_0. This indicates

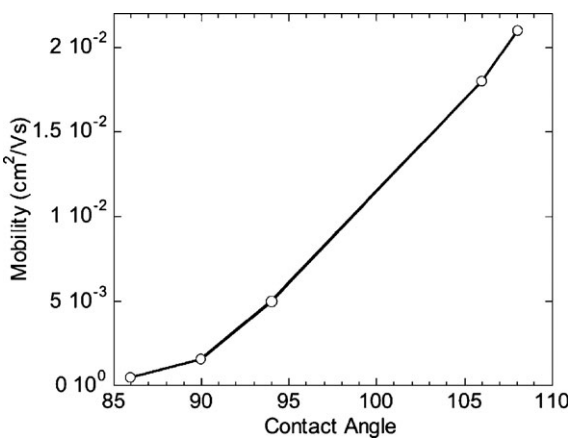

Fig. 4 Variation of the SAM FET saturation mobility with the contact angle of water on the SAM surface. Data points from left to right are for APTS, PETS, HMDS, OTS and ODTS.

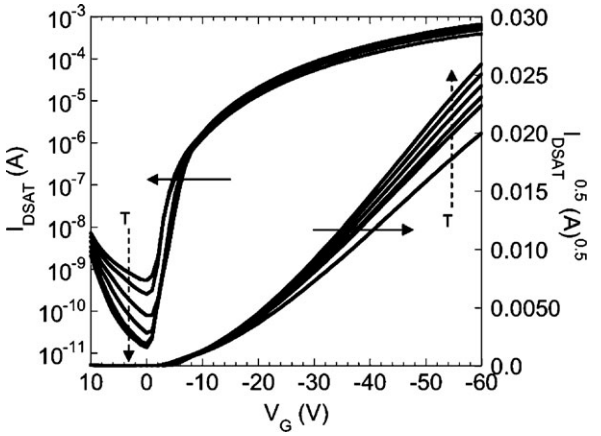

Fig. 5 Variation of the saturated regime transfer characteristics (at $V_D = -60$ V) with temperature T for the OTS treated polymer FETs ($L = 20$ μm). Vertical dashed arrows indicate the variation with T from 294 to 354 K in 10 K steps. The variation of the slope of $(I_D)^{1/2}$ *vs.* V_G indicates the variation of μ_{SAT}.

that the polymer semiconductor is pinned in depletion, it requiring a very large negative gate bias to swing the polymer into hole accumulation mode. PETS and APTS must therefore somehow introduce a large density of hole-trapping states at the interface, possibly as a result of increased disorder at the semiconductor/dielectric interface.

This is also consistent with the low mobility found for these two SAMs. Even when the devices are in accumulation mode and turned-on, holes are still being trapped at the interface as V_G becomes increasingly negative, hence giving a lower mobility. It also implies that these interface traps are distributed in energy above the crystalline HOMO levels.

The turn-on voltage for accumulation in a p-type organic FET is given by $V_0 = (\Phi_m - \Phi_s) - Q_{IS}/C_i - V_{inj}$, where $(\Phi_m - \Phi_s)$ is the difference in the semiconductor and metal workfunctions, Q_{IS} is the charge stored in any interface states, C_i is the insulator capacitance and V_{inj} the voltage drop due to injection at the source.[20] The values of V_0 for the OTS, ODTS, HMDS and reference devices suggest that $(\Phi_m - \Phi_s) - V_{inj} \approx 0$. We can therefore calculate an interface density of trapped holes at $V_G = 0$ of 1.0×10^{12} and 3.6×10^{12} cm^{-2} for PETS and APTS, respectively. This translates into about 1 and 4 trapped holes per 10 nm × 10 nm area at the SAM–polymer interface. In the same area there are about 400 SAM molecules and about 27 polymer chains (the latter estimate based on the packing and unit cell dimensions of the *ant* variant in FETs[15]). It therefore seems more likely that the traps are due to isolated chain defects at the edges or between the polymer crystallites rather than anything particular about the surface chemistry of PETS and APTS. This is consistent with these traps being distributed rather than at a single energy. It is also consistent with the results in Fig. 4, which implies that the factors which determine the mobility have the same root cause for all five SAMs.

Considering all of the above results for pBTCT, we would suggest that it is the polymer morphology at the buried interface which causes the differences in FET behaviour between the SAMs. This is rather than any particular chemical defects associated with PETS and APTS. The different wetting behaviour of the polymer formulation on the SAMs results in the formation of different levels of structure and order of the chains at the interface. This varies from ODTS with a high level of crystallinity and relatively little disordered material, to APTS with a low level of crystallinity and a relatively large amount of disordered material, the latter resulting in a large number of conformational chain defects at the interface which heavily trap charge.

The authors thank Merck Chemicals Ltd and the United Kingdom Engineering and Physical Research Council (GR/S14078/01) for supporting Ruth Rawcliffe.

Notes and references

1 S. R. Forrest, *Nature*, 2004, **428**, 911.
2 G. P. Collins, *Sci. Am.*, 2004, (August edn), 74.
3 M. Berggren, D. Nilsson and N. D. Robinson, *Nat. Mater.*, 2007, **6**, 3.
4 D. J. Gundlach, *Nat. Mater.*, 2007, **6**, 173.
5 J. Veres, S. Ogier, G. Lloyd and D. de Leeuw, *Chem. Mater.*, 2004, **16**, 4543.
6 R. J. Kline, M. D. McGehee and M. F. Toney, *Nat. Mater.*, 2006, **5**, 222.
7 S. Grecu, M. Roggenbuck, A. Opitz and W. Bruetting, *Org. Electron.*, 2006, **7**, 276.
8 D. H. Kim, Y. D. Park, Y. Jang, H. Yang, Y. H. Kim, J. I. Han, D. G. Moon, S. Park, T. Chang, C. Chang, M. Joo, C. Y. Ryu and K. Cho, *Adv. Funct. Mater.*, 2005, **15**, 77.
9 L. A. Majewski, R. Schroeder, M. Grell, P. A. Glarvey and M. L. Turner, *J. Appl. Phys.*, 2004, **96**, 5781.
10 Y. Wu, P. Liu, B. S. Ong, T. Srikumar, N. Zhao, G. Botton and S. Zhu, *Appl. Phys. Lett.*, 2005, **86**, 142102.
11 K. P. Pernstich, S. Haas, D. Oberhoff, C. Goldmann, D. J. Gundlach, B. Batlogg, A. N. Rashid and C. Schitter, *J. Appl. Phys.*, 2004, **96**, 6431.
12 G. Yoshikawa, J. T. Sadowski, A. Al-Mahboob, Y. Fujikawa, T. Sakurai, Y. Tsuruma, S. Ikeda and K. Saiki, *Appl. Phys. Lett.*, 2007, **90**, 251906.
13 Y. Jang, J. H. Cho, D. H. Kim, Y. D. Park and M. Hwang, *Appl. Phys. Lett.*, 2007, **90**, 132104.
14 M. Heeney, C. Bailey, K. Genevicius, M. Shkunov, D. Sparrowe, S. Tierney and I. McCulloch, *J. Am. Chem. Soc.*, 2005, **127**, 1078.
15 I. McCulloch, M. Heeney, C. Bailey, K. Genevicius, Iain MacDonald, M. Shkunov, D. Sparrowe, S. Tierney, R. Wagner, W. Zhang, M. L. Chabinyc, R. J. Kline, M. D. McGehee and M. F. Toney, *Nat. Mater.*, 2006, **5**, 328.
16 Y. Shen, M. W. Klein, D. B. Jacobs, J. C. Scott and G. M. Malliaras, *Phys. Rev. Lett.*, 2001, **86**, 3867.
17 H. Baessler, *Phys. Status Solidi B*, 1993, **175**, 15.
18 A. R. Inigo, H.-C. Chiu, W. Fann, Y.-S. Huang, U.-S. Jeng, T. L. Lin, C.-H. Hsu, K. Y. Peng and S. A. Chen, *Phys. Rev. B: Condens. Matter Mater. Phys.*, 2004, **69**, 075201.
19 T. Kreouzis, D. Poplavskyy, S. M. Tuladhar, M. Campo-Quiles, J. Nelson, A. J. Campbell and D. D. C. Bradley, *Phys. Rev. B: Condens. Matter Mater. Phys.*, 2006, **73**, 235201.
20 R. Rawcliffe, M. Shkunov, M. Heeney, S. Tierney, I. McCulloch, S. Khodabakhsh, T. Jones and A. J. Campbell, *Adv. Funct. Mater.*, submitted.